Conference Paper

Increasing Energy Efficiency of Electric Arc Foundry Furnaces

S. Timoshenko[1], M. Gybinskyi[2], Yu. Yaroshenko[3], and T. Vvedenska[4]

[1]Donetsk National Technical University, Pokrovsk, Ukraine
[2]National Metallurgical Academy of Ukraine, Dnepropetrovsk, Ukraine
[3]Ural Federal University (UrFU), Ekaterinburg, Russia
[4]NTU 'Dnipro Polytechnic', Dnepropetrovsk, Ukraine

Abstract

A set of low-cost energy-efficient solutions for electric arc furnaces (EAF) of a foundry class is proposed: 'deep' bath, water-cooled panels with a spatial structure, a system of dispersed aspiration. Numerical simulations of thermal operation and gas-dynamics for 3-ton EAF in conditions of long downtime show the possibility of reduction energy consumption by 6.5–9%, fugitive emissions by 2 times, melting dust removal from the EAF by 19% and significant lowering of specific refractory and electrodes expenditure.

Keywords: electric arc furnace, heat exchange during downtime, energy efficiency, bath geometry, water-cooled elements with a spatial structure, a system of dispersed aspiration

Corresponding Author:
S. Timoshenko
stimoshenko155@gmail.com

Received: 6 June 2018
Accepted: 15 June 2018
Published: 17 July 2018

Publishing services provided by Knowledge E

© S. Timoshenko et al. This article is distributed under the terms of the Creative Commons Attribution License, which permits unrestricted use and redistribution provided that the original author and source are credited.

Selection and Peer-review under the responsibility of the TIM'2018 Conference Committee.

OPEN ACCESS

1. Formulation of the Problem

In the foundries of machine-building plants an electric arc furnaces (EAF) with a capacity of 3–6 tons are widely used. Low capacity of transformer, power-consuming classical technology, inefficient aspiration system and long (up to 24 hours and more) downtime, predetermine their low energy efficiency in comparison with the EAF of a 'large' metallurgy. An urgent task is the development of low-cost energy-efficient solutions for the foundry class EAF modernization. Proposed solutions are justified by methods of numerical modeling.

2. Analysis of Recent Research and Publications

Processes of heat and mass transfer in the least energy efficient liquid bath period of the heat in many respects determine the technical and economic parameters of the EAF of a foundry class. D. Guo and G. Irons [1] found that about 80% of the arc energy

is transmitted to the bath by radiation, 15–18% by thermal conductivity and 2–5% is lost in the electrodes. J-C. Gruber, T. Echterhof and H. Pfeifer [2] investigated the effect of the high-temperature arc region on the formation of gas flows in the EAF, estimated the energy losses with cold air inflow and the temperature distribution of the radiating electrodes surface. O. Gonzales, M. Ramirez-Argaez and F. Conejo [3] showed that the rate of heating of the liquid bath by electric arcs increases with increasing arc length. The heat and mass transfer in the steelmaking bath, according to the studies of M. Kawakami, R. Takatani, L. Brabie [4], and J. Li and N. Provatas [5], are determined by the intensity of forced mixing of the melt and the magnitude of the interfacial surface. More complex mathematical models of V. Logar, D. Dovžan, I. Škrjanc [6]; F. Opitz and P. Treffinger [7]; A. Stankevich, V. Timoshpol'skii et al. [8] describe not only the processes in a liquid bath, but also, with certain assumptions, the melting dynamics of the charge by the energy of arc radiation.

The mentioned models describe the processes in rhythmically working EAF, in which heat accumulation by the lining do not exert a noticeable influence on the energy-technological indicators. At the same time, after a daily downtime of the foundry class EAF, according to [9], only to restore the lining enthalpy is required energy, close to theoretical consumption for steelmaking process.

The problem of increased heat loss by radiation the bath surface is aggravated by traditional views of technologists about a shallow and flat steel-smelting bath in the EAF to ensure the refining of steel on metal-slag interface [10].

Traditional for the foundry class EAF off-gas removal system through electrode clearances (portal chamber) is characterized by low efficiency of the off-gas emissions localization and significant air inflow into the furnace. The consequence is an elevated loss of the charge in form of melting dust (up to 20–22 kg/t) and electrodes, environmental problems, which increase with the wear of electrodes pinch zone that limits the overall lifetime of the roof [11].

In the foundry furnaces, the concept of water-cooled elements (WCE) application has not yet developed, as an economical substitute for the refractory lining, which is generally accepted in 'large' metallurgy EAF, operating with intensive technology. For example, in the USA only 12% of the foundry class EAF is equipped with WCE [12]. For given class of furnaces it seems rational a combined solutions of cooled and refractory elements, such as an energy efficiency compromise.

Thus, thermal operation of the refractory lining, charge and WCE in the period of downtime; heat and mass transfer processes and steelmaking bath geometry; gas dynamics of aspiration system should be reflected in the mathematical model and

taken into account in the implementation of energy-efficient solutions for foundry class EAF.

3. The Purpose

The research is aimed in the developing of low-cost solutions for improving the energy efficiency of foundry class EAF on the basis of numerical modeling of thermal operation and gas dynamics of the furnace.

4. The Main Part

A scheme, reflecting heat and mass transfer and gas dynamics in the working space of the EAF and solutions for increasing energy efficiency are shown in Figure 1. The researches were carried out with reference to 3 tons AC EAF with the capacity of the transformer 1.8 MVA.

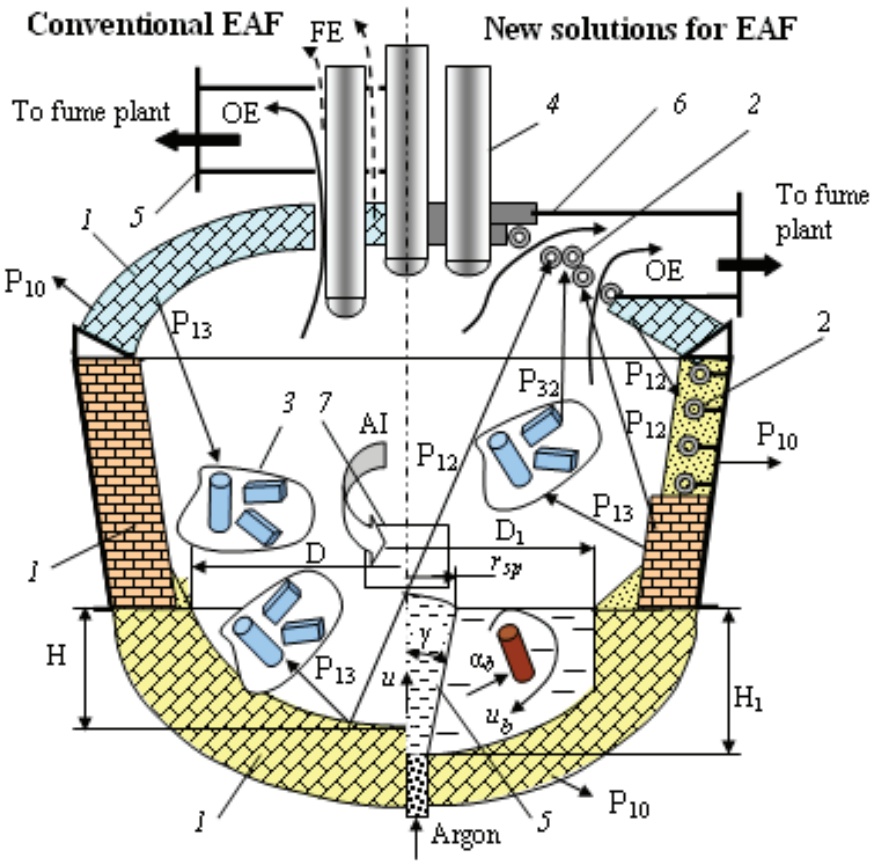

Figure 1: Scheme of heat exchange and aspiration in low-capacity EAF: 1 = refractory lining; 2 = wall and roof WCE; 3 = charge; 4 = electrodes; 5 = conventional aspiration system; 6 = system of dispersed aspiration; 7 = slag door; 8 = liquid bath; 9 = two-phase area; 10 = porous plug, 11 = fragment of scrap; OE, FE, AI = organized, fugitive emissions, air inflow, respectively. Other notations are given in the text.

4.1. Heat exchange in downtime

Two cases of thermal operation of the furnace in downtime are considered: with the charge in the working space for the next heat and without it (if uncertainty of the steel grade being melted after downtime). For each case, the next options are provided: conventional EAF with refractory lining (no WCE) and EAF partially with WCE. The second option assumes two variants of WCE: traditional with a dense pipes structure and energy-saving with a spatial pipes structure [13]. The relative area of the walls WCE, according to the conditions of safe operation, is fixed by the value 0.4; relative area of the roof WCE β_r varies from 0 to 1 for both variants. For the EAF with energy-saving WCE the option of bath geometry was assessed, as conventional 'shallow' and 'deep' (at equal mass) bath; for other options – 'shallow' bath.

The change in the lining enthalpy dQ during the EAF downtime τ_d is described in a one-dimensional setting by the following equation:

$$dQ/d\tau_d = P_{10} + P_{12} + P_{13}, \tag{1}$$

where P_{10}, P_{12}, P_{13} are power loss of energy from the EAF outer surface to the environment, and from the inner surface to WCE and charge, respectively (see Figure 1). Parameter P_{10} includes the radiation and convective components:

$$P_{10} = \alpha_{out}(T_s - T_0) + \sigma\epsilon_s(T_s^4 - T_0^4)F_s, \tag{2}$$

where σ is Stefan–Boltzmann constant; ϵ_s, F_s are emissivity and area of the casing outer surface, respectively, T_s, T_0 are temperatures of casing outer surface and environment, respectively.

The heat transfer coefficient of the casing outer surface to the environment α_{out} in (2) is determined by the equation [13], in which the expression under the logarithm is an empirical dependence between T_s and τ_d, obtained by processing the experimental data [9]:

$$\alpha_{out} = 31.46\ln(200 - 3.85 \cdot \tau_d) - 120.80. \tag{3}$$

The charge (scrap), if available in the furnace, when heated by energy of lining, transfers part of the heat P_{32} (see Figure 1) to WCE, that is taken into account in the process, described by (1), through the current scrap temperature. Engineering calculation of aforementioned P_{12}, P_{13}, P_{32} conducted with only radiation component by expression,

similar to (2), with regarding to the scrap and WCE temperatures, inner EAF surface and surface fraction of WCE.

4.2. Heat loss with cooling water in view of bath geometry and WCE option

The liquid bath period of the heat is considered, as the most heat-stressed. The model of heat exchange by radiation in the EAF, adapted to the assessment of influence the bath geometry on heat loss with cooling water [14], is shown in a Figure 2.

The resultant heat flux on the WCE is a function of the mutual radiation of bath, electrodes surfaces and the gas–dust environment in the working space, accounted by the reduced emissivity factor ϵ_r [15] in Stefan–Boltzmann equation for the power Q_{rad}, irradiating by the source surface S_{rad} with temperature T_{rad} per unit of the receiving surface with temperature T_{rec}:

$$Q_{rad} = \sigma \cdot \epsilon_r \cdot (T_{rad}^4 - Ó_{rec}^4) \iint_{S_{rad}} [(\cos\theta \cdot \cos\gamma)/r^2] \cdot dS_{rad}. \quad (4)$$

The arc radiation is screened by slag foam and is taken into account indirectly through the bath surface temperature. The power of heat loss of radiation energy by the heat-receiving surface S_{rec} is:

$$Q_{loss} = k_{av} \int_{S_{rec}} Q_{rad} \cdot dS_{rec}. \quad (5)$$

The averaging factor of the resulting heat flux k_{av} along the cooled surface of energy-saving WCE with developed slag lining, included in (5), was estimated on the basis of the calculation of stationary two-dimensional heat exchange problem in the WCE, performed in the ELCUT 6.2 software package, using the procedure and boundary conditions [13]. Results, shown in a Figure 3, touch energy-saving solutions with a spatial pipes structure: roof panels with displaced axes of pipes and wall panels with rare tubes [13]. For traditional WCE with a dense tube structure k_{av} is close to 1. The values of k_{av} for the roof and wall panels are 0.63 and 0.59, respectively (Figure 3c).

Modern means for bottom purging of the melt by inert gas allow compensating the decrease of interfacial surface by more intensive mixing of the reacting phases. In this case, it becomes possible to reduce the radiating area of the bath and, respectively, heat loss with cooling water by increasing the depth of the bath.

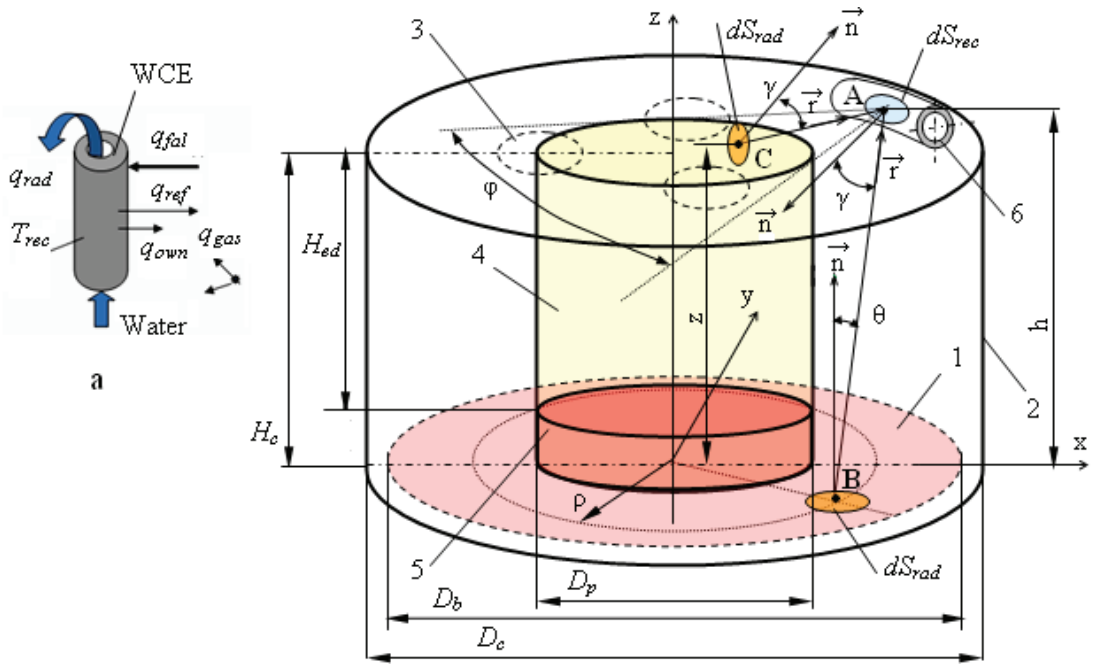

Figure 2: Resultant heat flux q_{rad} on WCE (a): q_{fal}, q_{ref}, q_{gas}, q_{own} = falling, reflecting and own heat flux, respectively. Scheme of radiation heat transfer in the EAF (b):1 = bath with diameter D_b; 2 = casing with diameter D_c and height H_c; 3 = electrode;4 = conditional electrodes surface with pitch diameter D_p and length H_{ed}; 5 = conditional arcs region; 6 = WCE; ρ, z, h = coordinates of receiving A point and radiation source B, C points; θ, γ, φ = guiding angles; $\vec{r}, \vec{n}$ = radius and normal vectors.

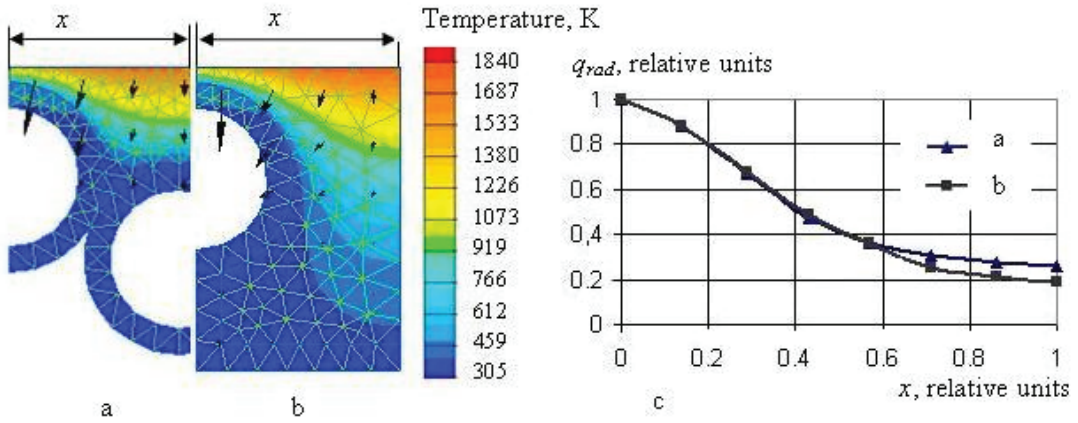

Figure 3: Temperature field in the roof WCE (a) and the walls WCE (b). Evaluation of average resultant flux of the heat loss with cooling water (c). Arrows show the direction of heat flux.

Option of a 'deep' bath can be realized without noticeable structural changes in the furnace by reducing the diameter of the radiating surface of the melt from D = 2.1 to D_1= 1.8 m (see Figure 1). In this case, the depth of the bath H_1 with respect to the initial H increases, at given melt mass, by about 35%. The calculated specific heat loss with cooling water, obtained by numerical solution (4), (5) in Mathcad 14.0 software package for initial conditions: melt mass 3 tons, duration of liquid bath conditional period 1.2 hours, are shown in Figure 4. According to calculations, the loss of heat with

water by using energy-saving WCE with a spatial structure is reduced by 37–39% in comparison with traditional panels with a dense structure of pipes. The 'deep' bath additionally reduces the energy loss by 13–18%.

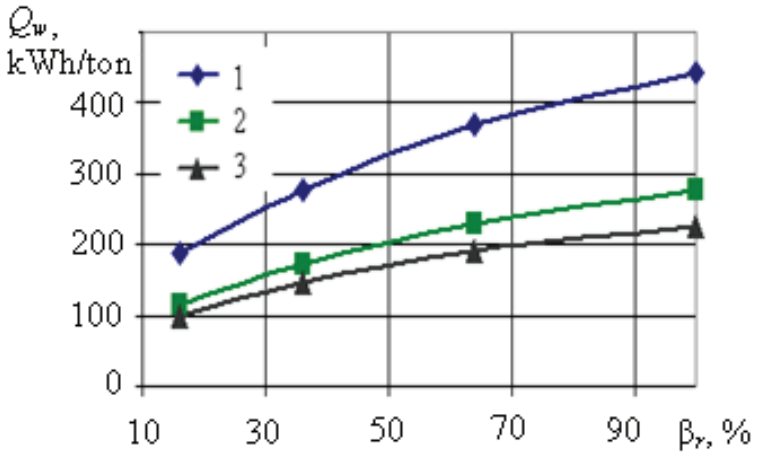

Figure 4: Specific energy loss with cooling water Q_w versus relative cooling area of the roof β_r: 1 = traditional WCE, 2 = WCE with spatial structure, 3 = WCE with spatial structure + 'deep' bath.

The advantage of a 'deep' bath is the intensification of heat and mass transfer processes in liquid steel. Let's evaluate the duration of melting of scrap fragments in a pneumatically stirred EAF bath. The driving force of the emerging metal circulation is the difference in the density of the medium in two-phase region with opening angle γ and argon-blowing 'spot' radius r_{sp} (see Figure 1) and of the surrounding space. According to [4], the following criteria equation describes the heat transfer in a liquid bath:

$$Nu = 0.017 \cdot Re^{0.8} \cdot Pr^{0.33}, \quad (6)$$

where $Nu = \alpha_b \cdot H/\lambda$ is Nusselt number; α_b is convective heat transfer coefficient in liquid bath; H is depth of the bath; λ, ν, ρ, C are heat conductivity, kinematic viscosity, density and heat capacity of liquid steel, respectively; $Re = u_0 \cdot H/\nu$ is Reynolds number; $u_0$is characteristic velocity of liquid bath; $Pr = \rho \cdot C \cdot \nu \ /\lambda$ is Prandtl number.

The main parameter determining α_b and, consequently, the intensity of melting of the scrap fragments in the bath, is the characteristic velocity in the liquid bath. Pneumatic mixing of the bath provides ascending flow in two-phase region and descending one in periphery (see Figure 1). According to D. Mazumdar, R. Guthrie and A. Ghosh [16, 17], the average melt velocity of mentioned flows u and u_b are the functions of

inert gas flowrate *G* and the geometric parameters of the bath *D*, *H* and determined by empirical equations:

$$u = 4.5G^{0.33} \cdot H^{0.25}/(0.5D)^{0.33}; \quad (7)$$

$$u_b = 0.79G^{0.33} \cdot H^{0.25}/(0.5D)^{0.67}. \quad (8)$$

In estimating α_b from (6), should take as the characteristic velocity in the liquid bath u_0 the weighted average of (7) and (8) with account the volumes of the two-phase and peripheral regions. For usual in given conditions value of α_b >10^4 W/(m^2·K) [5], is possible to assume for the main categories of lightweight scrap that the process of freezing and subsequent melting of the crust will not occur [18], and use the engineering method [19] to calculate the melting time τ_m:

$$\tau_m = (\xi \cdot \tilde{N}_{skr}/\alpha_{con}) \cdot \ln((T_b - \grave{O}_{scr})/(T_b - \grave{O}_m)), \quad (9)$$

where ξ is ratio of scrap fragment mass to its surface; C_{scr} is heat capacity of scrap; T_b, T_m, $T_{scr}$are temperature of bath, melting and scrap initial temperature, respectively.

The estimation of the melting rate of scrap in the EAF, performed according to (9) for typical scrap A3 with a bulk density of 0.7–0.8 ton/m^3, is shown in Figure 5.

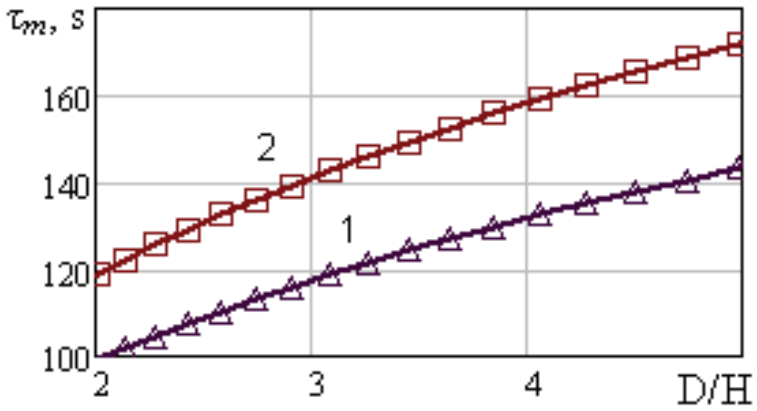

Figure 5: Scrap melting time τ_m, versus bath geometry ratio D/H. Inert gas purging rate 20 (1) and 40 Nm^3/h (2).

The results of the calculation agree with the experimental data of J. Li and N. Provatas [5] and show that the transition from a standard bath [10] with D/H = 4.5–5 to a 'deep' bath with D/H = 2.5–3 allows to increase the melting rate of scrap and, accordingly, the productivity and energy efficiency of the liquid bath period in EAF operation route by 12–20%.

4.3. System of dispersed aspiration

Innovation, based on the principles of dispersing the suction surface and approaching it to electrode clearances, suggested with the goal of reducing fugitive emissions and air inflow [20]. Structurally the system of dispersed aspiration designed in form of a roof chamber with a horizontal off-gas duct connected by an additional channel to the periphery of the sub-roof space (see Figure 1).

Preliminary analysis show, that the medium flow in the object under study, is turbulent (Re = 10^5). Numerical simulation was performed on the basis of Navier–Stokes (10) and continuity (11) equations using the k-ε turbulence model in 'CosmosFloWorks' software package.

$$\frac{\partial \vec{w}}{\partial \tau} + (\nabla \vec{w}) \cdot \vec{w} = -\frac{1}{\rho} \cdot \nabla p + \eta \cdot \nabla^2 \vec{w} + F; \tag{10}$$

$$\text{div } \vec{w} = 0, \tag{11}$$

where ρ is density, w is velocity, p is pressure, τ is time, F is volumetric density of forces, η is dynamics viscosity coefficient of medium.

Calculation of the field of velocities, pressures and temperatures of the gas flow in the model of 3-ton foundry class AC EAF was carried out under the following assumptions and boundary conditions adopted in the model [20]: the melting period is considered; air is taken as the working gas; heat exchange of gas with elements of the working space is absent; outlet section of the off-gas duct under pressure is 15 Pa, average temperature of the exhaust gases is 1000 K; in the section of the slag door and on the surface of conditioned chamber above the furnace are normal conditions: atmospheric pressure and gas temperature 293 K; at the bottom of the 'well', melted by arcs in the burden, the gas flowrate is 2 m^3/s at temperature 1850 K and atmospheric pressure; electrode clearances are 30 mm; other surfaces – the real wall.

The results of numerical calculation the velocity field were superimposed on the flow of fusion dust particles, generated by a conditional source of gas–dust flow in mentioned earlier 'well'. The dust emission parameters, adopted in the numerical model are: intensity 0.042 kg/s, average particle size 20 μm, density 3 g/cm^3 correspond to the data [21]. The number of conditional dust particles in the formation zone of the 'well' is assumed to be 100. The velocity and temperature of the dust particles in the numerical model are tied to the calculated parameters of the gas flow.

The results of numerical modeling in the form of a velocity field with the tracks of melting dust, superimposed on it, are shown in a Figure 6. The general picture of gas dynamics in the working space of the furnace indicates a more effective localization of fugitive emissions using a dispersed gas removal system, as can be seen from the number of tracks of dust particles passing through the electrode clearances into the space of the conditional chamber above the roof.

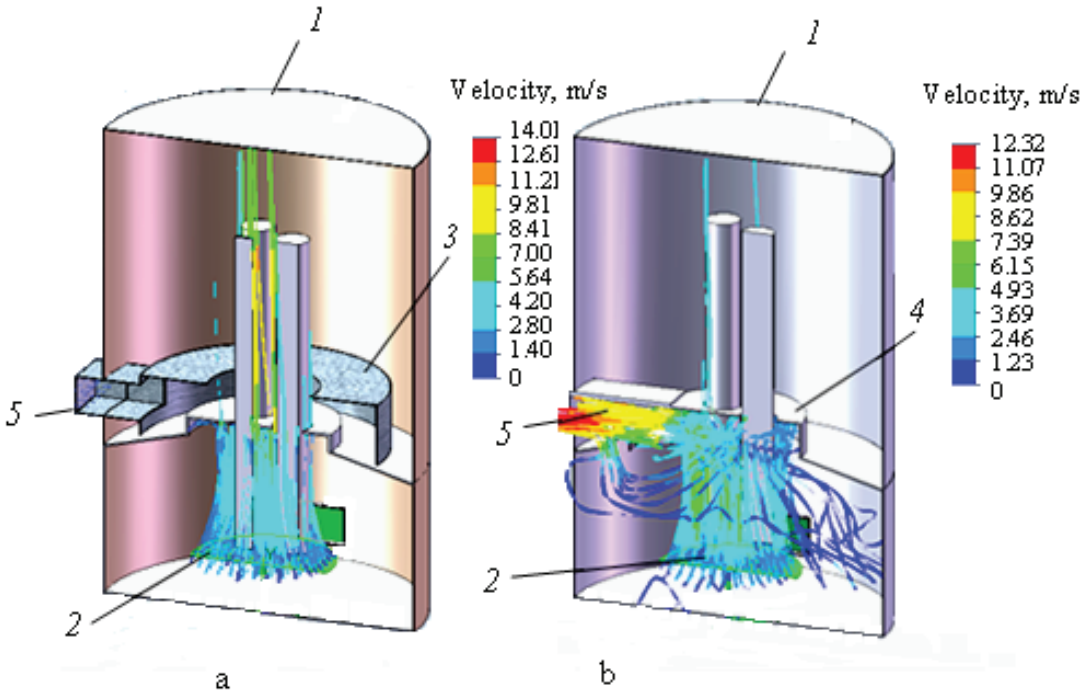

Figure 6: Velocity field and streamlines of the gas–dust flow in the model of 3-ton EAF:a = traditional aspiration system; b = system of dispersed aspiration. 1 = conditional chamber; 2 = conditional surface, generating gas–dust flow; 3 = portal chamber; 4 = roof chamber; 5 = off-gas duct.

The integral values of the parameters characterizing the quality of the aspiration system, obtained as a result of solving the problem, are given in Table 1.

Table 1: Evaluated performance indicators for aspiration systems of 3-ton EAF.

Option in Figure 6	The fraction of fugitive emissions in total flow, %	The fraction of air inflow in total flow, %	The fraction of dust particles, removing from the EAF, %		
			In electrode clearances	In off-gas duct	Total
a	37.2	18.2	42	0	42
b	18.4	16.3	2	32	34

The simulation results show a low efficiency of the portal chamber when fugitive emissions are captured through electrode clearances, which constitute 37% of

the total off-gas flow. The situation with removal of melting dust from the furnace, which reaches 42% of its total amount, formed during the melting of the charge, is unsatisfactory. At the same time, the portal chamber provides a relatively small influx of air, which is associated with an increased hydraulic resistance to the movement of furnace gases. Streamlines of conditional dust particles (Figure 6a) confirm the aforementioned.

The use of a system of dispersed aspiration instead of a traditional portal chamber leads to a reduction of fugitive emissions by 2 times, an air inflow to the furnace by 11%, and removal of melting dust from the furnace by 19%.

4.4. Energy efficiency of the set of new solutions

The estimation of (1), performed numerically in Mathcad 14.0 software package, yields the energy consumption on heat accumulation by the enclosing of EAF working space (lining, WCE), as a function of β_r and τ_d. These data used to assess the energy efficiency of proposed solutions for modernization, which constitutes in comparison the specific electricity consumption for two mentioned cases (downtime with charged scrap and without it) for conventional EAF (Qel_1) with refractory lining and a new solutions of the EAF with aforementioned options of WCE and bath geometry (Qel_2). In view of the comparative nature of the evaluation, in the energy balance of the EAF a number of consumables (heat loss through the lining, electrical loss), as well as the input constituents (heat of exothermic reactions) are assumed to be the same for the considered cases and options. These items estimated, as usual practice, according to [22]. In evaluation the theoretical energy consumption for heating and melting the charge, overheating of the melt to tapping temperature, slag formation and alloying, the residual enthalpy of scrap was taken into account.

Ratio $\chi = Qel_2/Qel_1$, which is criteria of energy efficiency of proposed solutions, is presented in Figure 7 depending on downtime duration τ_d and relative cooling area of the roof β_r.

According to the presented data, in a small capacity EAF of a foundry class for a duration of downtime up to 15–20 hours and more, energy consumption for accumulation of heat, dissipated by the refractory lining, makes energy-efficient the solution of partial replacement the refractory by WCE of a spatial structure (use of traditional WCE is not effective) jointly with the 'deep' bath.

For a short downtime (up to 1 hour), pre-charge of the EAF equipped with WCE reduces the energy efficiency of the unit in comparison with refractory lined furnace

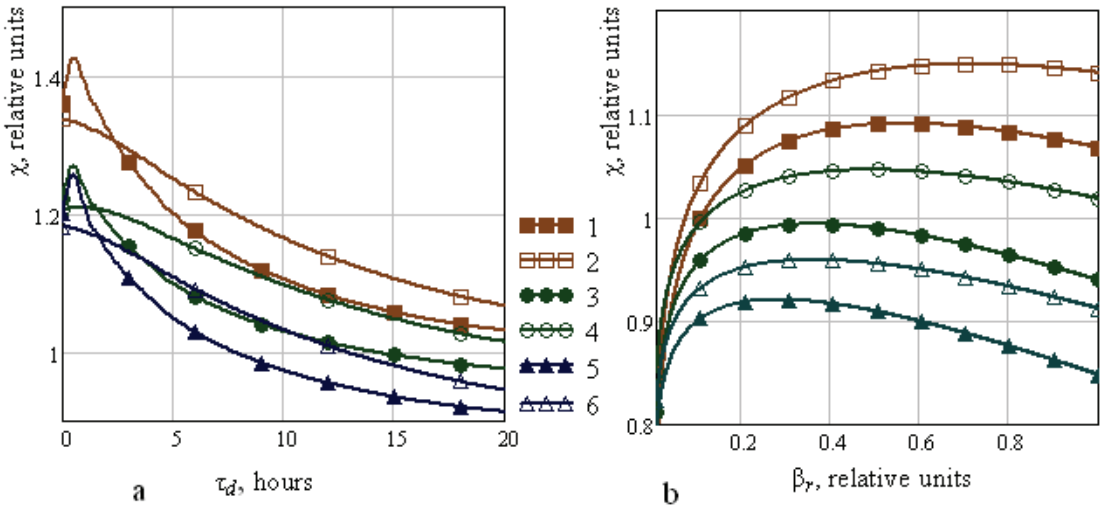

Figure 7: Energy efficiency of proposed solutions χ: a = versus downtime τ_d; b = versus relative cooling area of the roof β_r at τ_d = 20 hours. 1and 2 = traditional WCE with and without scrap, respectively; 3 and 4 = energy-saving WCE with and without scrap, respectively; 5 and 6 = energy-saving WCE + 'deep' bath with and without scrap, respectively.

(see Figure 7a), since scrap heated by the lining emits part of the energy to theWCE, and the lining does not largely lost the initial enthalpy. For a longer downtime, the presence of scrap into workspace increases the energy efficiency of the EAF due to lowering heat loss of the refractory lining by screening WCE and due to corresponding reduction of the energy consumption for accumulation of the lining heat, as well as by utilization of the enthalpy of heated scrap in the steelmaking process. In general, the preliminary loading of scrap into the furnace increases the possibilities of considered solutions for the EAF modernization, both in the direction of reducing the threshold for the downtime duration, and the rationality of increasing the relative area of WCE.

For the case of EAF, using energy-saving panels and a 'deep' bath, with downtime more than 20 hours, an energy-efficient operation even with fully water-cooled roof is possible (see Figure 7b). However, taking into account the possible and desired reduction in downtime, for a small EAF of a foundry class a roof with a relative cooling area of up to 0.2–0.25 should be recommended.

5. Summary

According to numerical modeling of the thermal work and gas dynamics of 3-ton foundry class EAF operating with downtimes of 15–20 hours, increasing the depth of the steelmaking bath by about 35% and introduction the roof and walls WCE with relative area of 20–25% and 40%, respectively, provide 6.5–9% energy savings is

steelmaking route due to lower heat consumption for accumulation of enthalpy by massive refractory lining and heat loss by radiation.

The system of dispersed aspiration reduces fugitive dust and gas emissions through electrode clearances by 2 times, and the removal of melting dust from the furnace by 19%.

The main effect of the proposed solutions implementation is in significant reduction of the refractory and electrodes consumption due to replacement of brick by WCE and decrease the intensity of furnace gases washing of graphite surface in process of aspiration.

References

[1] Guo, D. and Irons, J. (10–12 December 2003). Modeling of radiation intensity in an EAF. *Third International Conference of CRD in the Minerals and process industry*, pp. 223–228. Melbourne, Australia: CSIRO.

[2] Gruber, J., Echterhof, T., and Pfeifer, H. (2016). Investigation on the influence of the arc region on heat and mass transport in an EAF freeboard using numerical modeling. *Steel Research International*, vol. 87, no.16, pp. 15–28.

[3] Gonsalez, O., Ramirez-Argaez, M., and Conejo, A. (2010). Effect of arc length on fluid flow and mixing phenomena in AC electric arc furnaces. *ISIJ International*, vol. 50, no. 1, pp. 1–8.

[4] Kawakami, M. and Takatani, R. (1999). Heat and mass transfer analysis of scrap melting in steel bath. *Tetsu to Hagane*, vol. 85, no. 9, pp. 658–665.

[5] Li, J. and Provatas, N. (2008). Kinetics of scrap melting in liquid steel: Multipiece scrap melting. *Metallurgical and Material Transactions*, vol. 39B, no. 4, pp. 268–279.

[6] Logar, V., Dovžan, D., and Škrjanc, I. (2012). Modeling and validation of an electric arc furnace. *ISIJ International*, vol. 52, no. 3, pp. 402–423.

[7] Opitz, F. and Treffinger, P. (2016). Physics-based modeling of electric operation, heat transfer, and scrap melting in an AC electric arc furnace. *Metallurgical and Material Transactions*, vol. 47, pp. 1489–1503.

[8] Stankevich, Yu. A., Timoshpol'skii, V. I., Pavlyukevich, N. V., et al. (2009). Mathematical modeling of the heating and melting of the metal charge in an electric arc furnace. *Journal of Engineering Physics and Thermophysics*, vol. 82, no. 2, pp. 221–235.

[9] Mironov, Yu. M. and Petrov, V. G. (2010). Thermal losses and power efficiency of arc steelmaking furnaces. Metally (Russian Metallurgy), no. 12, pp. 1141–1144.

[10] Egorov, A. V. (1990). Raschet Moschnosti I Parametrov Elektropecej Chernoj Metallurgii [Calculation of Power and Parameters of Electric Furnaces of Ferrous Metallurgy], p. 280. Moscow: Metallurgija (in Russian).

[11] Doroshenko, A. V., Djad'kov, B. P., Timoshenko, S. N., et al. (2017). Kombinirovanniy vodookhlazhdayemyy svod dugovykh elektropechey maloy vmestimosti [Combined water-cooled roof of electric arc furnaces of small capacity]. Metallurgicheskaya i gornorudnaya promyshlennost' [Metallurgical and mining industry], no. 5, pp. 91–95 (in Russian).

[12] Biswas, S., Peaslee K., and Lekakh S. Melting Energy Efficiency in Steel Foundries/AFS Transactions 2012 © American Foundry Society, Schaumburg, IL USA, pp. 449–456. Retrieved from http://www.afsinc.org/files/12-040.pdf (assessed on 07 March 2018).

[13] Timoshenko, S. N., Filippi, A. A., Onischenko, S. P., et al. (2017). Energoeffectivnye reshenija pri modernizatsii dugovykh pecei postojannogo toka liteinogo klasssa [Energy efficient solutions for modernization of foundry class DC EAF]. Metall i lityo Ukrainy [Metal and Foundry of Ukraine], no. 8–10(291–293), pp. 48–55 (in Russian).

[14] Timoshenko, S. N. (2016). Computer modeling bath geometry to improve energy efficiency of electric arc furnace/ *System Technologies*. Regional interuniversity collection of scientific works. *Dnipro*, vol. 3, no. 104, pp. 33–39.

[15] Howell, J., Pinar Menguc, M., and Siegel, R. (2011). Thermal Radiation Heat Transfer (5th edition) p. 987. Boca Raton, London, New York: CRC press and Taylor & Francis Group.

[16] Mazumdar, D. and Guthrie, R. I. L. (1995). The physical and mathematical modeling of gas stirred ladle systems. ISIJ International, vol. 35, no. 1, pp. 1–20.

[17] Ghosh, A. (2000). Secondary Steelmaking: Principles and Applications, p. 344. CRC Press.

[18] Serikov, V. A., Bikeyev, R. A., Cherednichenko, M. V., et al. (2015). Ugar metalla i nagrev shikhty v rasplave v dugovykh elektropechakh [Burning of metal and heating of batch in a melt in arc furnaces]. Elektrometallurgiya [Electrometallurgy], no. 9, pp. 2–8 (in Russian).

[19] Timoshenko, S. N. and Gubinski, M. V. (2016). Povysheniye energoeffektivnosti elektrostaleplavil'nogo protsessa s nepreryvnym plavleniyem shikhty v zhidkoy vanne [Increase of energy efficiency of electric steelmaking process with continuous melting of charge in a liquid bath]. Technical ThemoPhysics and Industrial Heat Engineering. Collection of scientific works/Dnipro: Nova Ideologia, vol. 8, pp. 174–183 (in Russian).

[20] Timoshenko, S. N., Tischenko, P. I., Timoshenko, N. S., et al. (2013). Modelirovaniye sistemy aspiratsii elektrodugovoy pechi s tsel'yu povysheniya energoeffektivnosti i ekologicheskoy bezopasnosti [Modeling of the electric arc furnace aspiration system to improve energy efficiency and environmental safety]. Ekologiya i promyshlennost' [Ecology and industry]. Kharkov: 'UkrNTC' Energostal„ vol. 2, no. 35), pp. 66–69 (in Russian).

[21] Guézennec, A., Huber, J., Patisson, F., et al. (2004). Dust formation by bubble-burst phenomenon at the surface of a liquid steel bath. ISIJ International, vol. 44, no. 8, pp. 1328–1333.

[22] Toulouevski, Yu. N. and Zinurov, I. Y. (2010). Innovation in Electric Arc Furnaces. Scientific Basis for Selection, p. 258. Berlin: Springer.